Non-contact Transportation of Flat Panel Substrate by Combined Ultrasonic Acoustic Viscous and Aerostatic Forces

Hiromi ISOBE[1,#], Masaaki FUSHIMI[2], Masami OOTSUKA[3] and Akira KYUSOJIN[4]

1Department of Mechanical Engineering, Nagano National College of Technology
2Business Generalization Division, Produce Co., Ltd
3Project Development Division, Produce Co., Ltd.
4Department of Mechanical Engineering, Nagaoka University of Technology
#Corresponding Author / E-mail: isobe@me.nagano-nct.ac.jp, TEL/FAX: +81-26-295-7054

KEYWORDS: Acoustic radiation, Noncontact transportation, Squeeze effect, Ultrasonic motor, Viscous flow

In recent years, the size of plane substrates and semiconductor wafers has increased. As conventional contact transportation systems composed of, for example, carrier rollers, belt conveyers, and robot hands carry these longer and wider substrates, the increased weight results in increased potential for fracture. A noncontact transportation system is required to solve this problem. We propose a new noncontact transportation system combining acoustic viscous and aerostatic forces to provide damage-free transport. In this system, substrates are supported by aerostatic force and transported by acoustic viscous streaming induced by traveling wave deformation of a disk-type stator. A ring-type piezoelectric transducer bonded on the stator excites vibration. A stator with a high Q piezoelectric transducer can generate traveling vibrations with amplitude of 3.2 μm. Prior to constructing a carrying road for substrates, we clarified the basic properties of this technique and stator vibration characteristics experimentally. We constructed the experimental equipment using a rotational disk with a 95-mm diameter. Electric power was 70 W at an input voltage of 200 Vpp. A rotational torque of 8.5 × 10^{-5} Nm was obtained when clearance between the stator and disk was 120 μm. Finally, we constructed a noncontact transport apparatus for polycrystalline silicon wafers (150(W) × 150(L) × 0.3(t)), producing a carrying speed of 59.2 mm/s at a clearance of 0. 3 mm between the stator and wafer. The carrying force when four stators acted on the wafer was 2 × 10^{-3} N. Thus, the new noncontact transportation system was demonstrated to be effective.

Manuscript received: May 1, 2006 / Accepted: December 18, 2006

1. Introduction

In recent years, the surface area of plane substrates and semiconductor wafers has continually increased. Transporting substrates with a conventional thickness but increased lengths and widths requires a delicate technique. It is difficult for conventional contact transport systems using, for example, carrier rollers, belt conveyers, and robot hands to prevent fracture caused by the substrate's own weight. In addition, as circuit integration technology advances, it is increasingly important to reduce particles that may be caused by contact between Si wafers and carriers, so a new noncontact transporting technology is required.

Researchers are currently investigating noncontact transport methods based on electrostatic forces[1] or acoustic radiation/viscous forces.[2-5] It is possible to use an electrostatic force to increase the load carrying capacity and carrying force by optimizing electrode construction and driving patterns. However, this kind of system is unstable, as are magnetic levitation systems, since they use electrostatic attractive forces. Therefore, a stabilization control system or on/off control system is necessary.

Acoustic radiation pressure levitates substrates and a viscous force moves them. This system works by utilizing the air between a substrate and a carrying road. The system does not allow any air possibly containing particles to flow in or out of the carrier road. The technique is extremely suitable for production processes requiring a high level of purity, but the system's load capacity is one order lower than that of contact and electrostatic force-type systems.

We propose a new noncontact transport system that uses a combination of acoustic viscous and aerostatic forces. Substrates are supported by aerostatic forces and transported by acoustic viscous flows induced by traveling wave deformation of a disk-type stator. This noncontact transport prevents the substrate from fracturing and subsequently fouling, increasing yield. Furthermore, the levitation force produced by the aerostatic pressure and the carrier force produced by the acoustic viscous force are proportional to the substrate's base area. Therefore, an increased substrate size results in an increased levitation force and carrier force. We evaluated stator performance by measuring the rotational

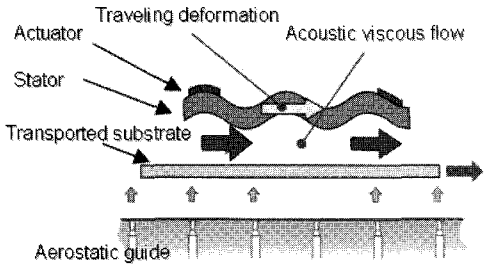

Fig. 1 Principles of noncontact transport

speed of a disk levitated by aerostatic pressure and acoustic radiation pressure. Furthermore, we successfully constructed a straight desktop transport system capable of carrying a 150(W) × 150(L) × 0.3(t) substrate.

2. Principles of Noncontact Transport

Ueha et al. conducted an elaborate and ingenious experiment and analysis of noncontact transport technology using acoustic viscous flow. In the present study, substrates levitate due to an aerostatic pressure, and an acoustic viscous flow excites the carrying force. As illustrated in Fig. 1, a ring-shaped piezoelectric actuator bonded to an aluminum disk stator generates deflection, which is propagated in the stator's circumferential direction. The deflection component in the stator's normal direction generates an acoustic radiation pressure, which pushes down on the stator, and the aerostatic pressure pushes up. Hence the substrate levitates in a stable, balanced position. Simultaneously, the deflection component in the circumferential direction produces an acoustic viscous flow near the substrate. This flow produces a carrying force. However, when the entire surface of a disk stator faces the substrate, the acoustic viscosity flow results in rotational torque rather than a straight carrying force. In this case, as shown in Fig. 2(a), stator half-faces, which are aligned on both sides of the carrying road, cover the substrate. If the propagation directions of the traveling waves differ from each other, the resultant force for a pair of stators is along the carrying road. This technique has the advantage of being able to produce various carrying patterns according to production process requirements. By aligning driving units (which consist of stators and piezoelectric actuators) along the carrying road, a substrate's carrying path can be easily modified. For example, Fig. 2 illustrates how any operation required during the transportation process can be achieved by constructing a carrying road and controlling driving units appropriately.

(a) Acceleration or deceleration condition, as shown in Fig. 2(a):
The operation pattern of each driving unit should be set to make the acoustic viscous flow have a resultant force in the transporting direction. Reversing the propagation direction of the traveling wave decelerates the substrate.

(b) Stationary state or constant velocity, as shown in Fig. 2(b):
When a constant velocity is required, the traveling wave of the flexure deformation stator should be set to a standing wave. As a result, the carrying force of each driving unit becomes zero. Otherwise, the resultant force affecting the substrate should be set at zero.

(c) Steering, as shown in Fig. 2(c):
The carrying force of the outside driving units can be increased and/or the force of the inside units can be decreased.

Complicated and flexible carrying road designs can be achieved by combining driving units.

3. Disk Rotation Test

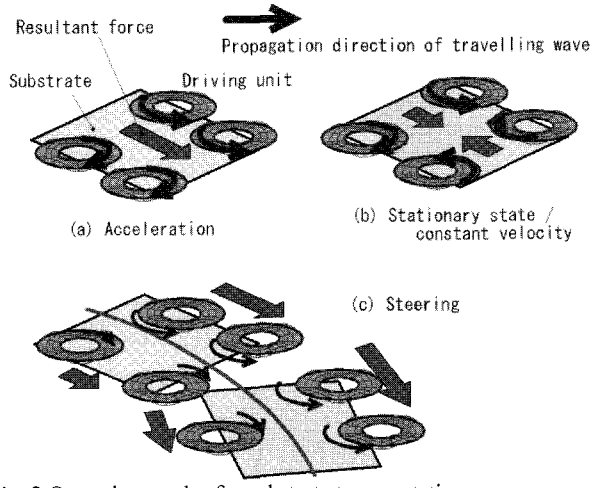

Fig. 2 Operation modes for substrate transportation

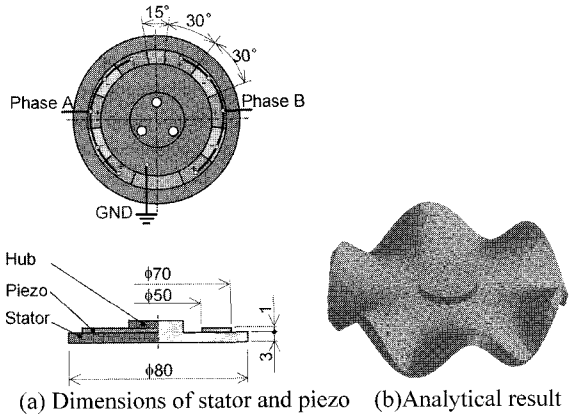

(a) Dimensions of stator and piezo (b)Analytical result

Fig.3 Design of stator with resonance frequency of 20.9kHz

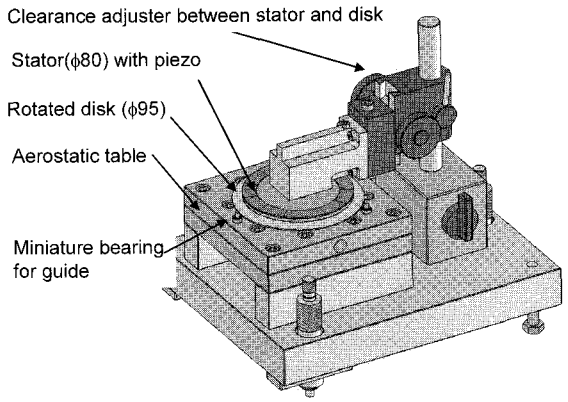

Fig.4 Experimental apparatus for disk rotation test

Before constructing a substrate carrying road, we experimentally clarified the basic properties of the proposed technique and the stator vibration characteristics using a rotational disk to simulate a substrate.

3.1 Stator design

The stator was a thin disk made of aluminum with a diameter of 80 mm and a thickness of 3 mm to facilitate the manufacturing process illustrated in Fig. 3(a). The central hub, which had a thickness of 6 mm, was bolted to a clearance adjustment stand. A finite elemental modal analysis was adapted to the aluminum stator (Young's modulus = 72 GPa; Poisson ratio = 0.33; density = 2680 kg/m^3). The results of this analysis, shown in Fig. 3(b), indicate that the stator had a deflection mode with six waves in the circumferential direction (B06 vibration mode) at the natural frequency of 20.9 kHz. The ring-type piezoelectric actuator had a

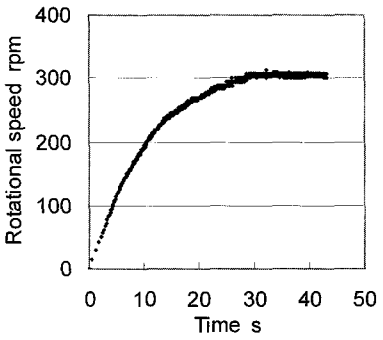

Fig. 5 Transient response of the rotational speed

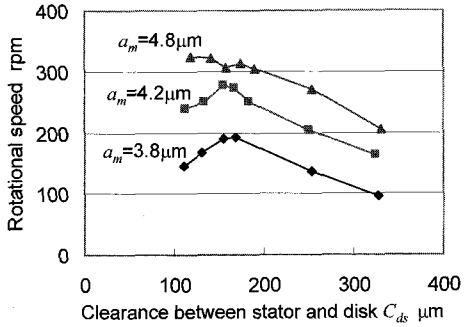

Fig. 6 Effect of the clearance between the disk and stator on rotational speed

φ70 outer diameter, a φ50 inner diameter, and a thickness of 1 mm. It was bonded to the stator's back surface by an epoxy resin hardened at room temperature. Phases A and B of the piezoelectric actuator were each divided into five electrodes. The arc angle of each electrode was one-half the wavelength (30°) of the flexural vibration wave. The piezoelectric actuator was polarized in the thickness direction, where + or – refers to the polarized direction. Phase A had a 15° spatial quarter phase difference of flexural vibration wave. Therefore, the stator resonated in deflection mode B06 and the deflection traveled in the circumferential direction when an AC voltage of 20.9 kHz was applied to phase A, and a voltage phase difference of 90° was applied to phase B. Resonance frequency was experimentally confirmed by determining the driving frequency in the vicinity of 20.9 kHz, when the maximum oscillation of deflection mode B06 was observed in the constructed stator.

3.2 Experimental apparatus

The apparatus illustrated in Fig. 4 levitated the disk using aerostatic pressure and rotated it with an acoustic viscous flow excited by a traveling wave from disk stator deflection. Clearance between the stator and the disk was defined as C_{ds}. The disk, a 3.5-inch magnetic disk taken from a hard disk drive, had a 95-mm radius, a 0.8-mm thickness, and a mass of 15 g; its moment of inertia was 1.7×10^{-5} kgm^2 and its surface roughness was 0.006 μmRa. The disk was supported by aerostatic pressure from the aerostatic table, and had a 'flying height' of about 0.3 mm at an exhaust pressure of 0.2 MPa and an airflow rate of 10 L/min. Three miniature ball bearings were installed on the aerostatic table to prevent the disk from 'dropping' on the table.

3.3 Rotational speed

Figure 5 shows the increase in the disk's rotational speed from a stationary state to terminal rotational speed. The experiment was based on the assumptions that the only force acting on the disk was rotational torque caused by acoustic viscous force, and that air resistance torque acting on the disk increased in proportion to the rotational speed. Therefore, the rotating speed start-up characteristic becomes a first-order differential equation involving terminal velocity. Figure 6 shows the influence of clearance between disk and stator on terminal rotating speed at vibrational amplitudes of a_m = 3.8, 4.2, and 4.8 μm. Clearly, a faster rotating speed coincided with larger vibration amplitude. At vibrational amplitude of 4.8 μm, the rotating speed increased with a decrease in clearance. However, at vibration amplitudes of 3.8 and 4.2 μm, the maximum rotating speed was produced at a clearance of 160 μm. This result indicates that the clearance between the transported substrate and stator was appropriate for achieving a faster carrying speed.

3.4 Torque

The carrying force or rotational torque transferred through the gas was so minimal that it was difficult to accurately measure the

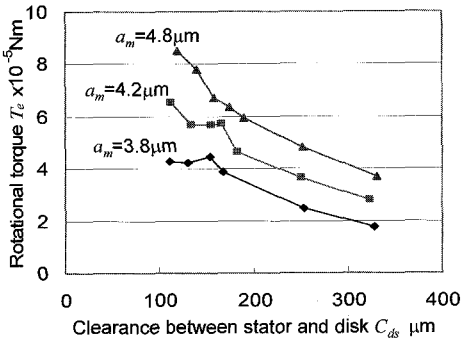

Fig. 7 Torque versus clearance between the disk and stator

torque produced by the acoustic viscous flow. Thus, the rotating torque was calculated from the rotating speed, as determined above.

Assuming that only viscous resistance (which is proportional to rotating speed) acts on a disk, the rotational torque can be calculated using the equation of rotational motion:

$$T = I\ddot{\theta} + C\dot{\theta}, \tag{1}$$

where T is rotational torque, I is the disk's moment of inertia, C is the viscous damping coefficient, $\dot{\theta}$ is the disk's angular velocity, and $\ddot{\theta}$ is the disk's angular acceleration. Viscous damping coefficient C was obtained by measuring the attenuation of rotational speed from terminal rotational speed when the stator's deflection traveling wave was switched to a standing wave. Deflection of a standing wave generated no rotational torque. We also observed that the damping coefficient increased with decreasing clearance between the stator and disk. Rotational torque was calculated from the time constant of the rotational speed transient response and the damping coefficient using Eq. (1). Figure 7 shows the relationship between rotational torque T and clearance C_{ds}. Here, vibration amplitudes were a_m = 3.4, 4.2, and 4.8 μm, respectively. Clearly, increasing vibration amplitude and decreasing clearance between the stator and disk resulted in greater rotational torque. Maximum rotational torque, 8.5×10^{-5} Nm, was produced when the vibration amplitude was 4.8 μm and the clearance was 120 μm.

4. Construction of the Carrying Road

4.1 Design of the carrying road

A straight noncontact carrying road with desktop dimensions was designed and constructed as shown in Fig. 8. The transported substrate was constructed of polysilicon wafers, each 150(W) × 150(L) × 0.3(t) with a mass of 16.5 g and a surface roughness of 2.1 μmRa. The driving unit consisted of a stator, a clearance adjuster, and an aerostatic table; it was mounted on a rigid flame rail to allow variation in pitch between the aerostatic table and driving units. The aerostatic table was made from porous ceramic; it had a flatness of

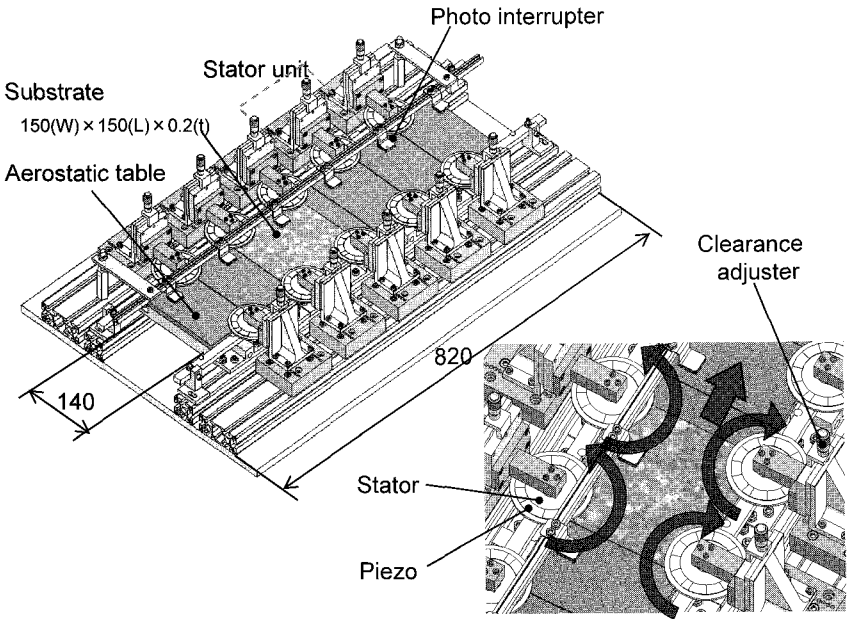

Fig.8 Desk top carrying road

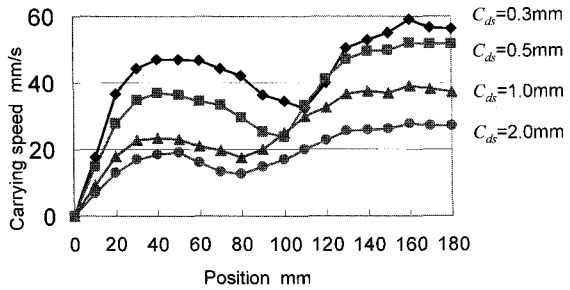

Fig. 9 Fluctuation of the carrying speed

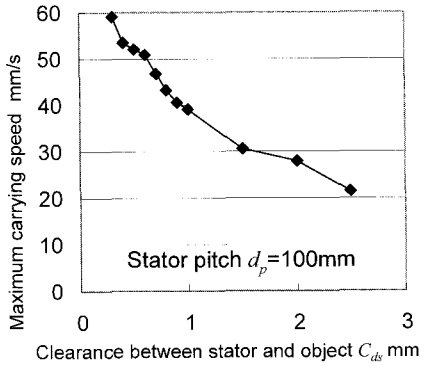

Fig.10 Maximum carrying speed

0.01 mm and an angle of inclination to the horizontal plane of 0.1 mm/m or less. Each aerostatic table unit had a flow rate of 10 L/min and an exhaust pressure of 0.2 MPa, and the substrate had a levitating height of 0.7 mm. Photo interrupters were installed above the aerostatic table unit. When an interrupter detects the substrate, the sequential controller stops the stator through which the substrate has just passed and drives the next stator in line to carry the substrate. Thus, transport is achieved by switching the driving to each stator depending on the position of the substrate being carried. To prevent the substrate from dropping out of the carrying road, pins with an outside diameter of 8 mm were installed as guides on both sides of the carrying road.

4.2 Carrying speed

Figure 9 shows the instantaneous carrying speed for a stator pitch of d_p = 100 mm. At the initial position, the first and second pair of stators provide the carrying force to the substrate. After movement begins, the first pair is turned off when the photo interrupter installed between the second and third pair of stators detects the substrate, and the third stator pair is turned on. Switching the piezo driving amplifier requires 1 s, during which time only the second stator works to carry the substrate. This causes a slight reduction in carrying speed, but the carrying speed increases again as third pair is driven.

Figure 10 illustrates the dependence of the maximum carrying speed on clearance between the stator and substrate. The carrying speed increases with decreasing clearance, likely because a greater acoustic viscous force is generated when a stator is nearer the substrate. However, when the whole stator surface faces the substrate, the viscous resistance increases compared to the acoustic viscous force (as discussed with regard to disk type apparatus in Section 2). Therefore, an excessively close proximity between the stator and substrate appears to result in a decreased carrying speed.

5. Conclusions

We constructed basic experimental equipment using a rotational disk to clarify stator vibration characteristics and the basic properties of a noncontact transport mechanism. The amplitude of the stator deflection traveling waves increased the rotational torque generated by the acoustic viscous flow. An appropriate clearance between the stator and rotating disk (which corresponded to the transport system's carried substrate) resulted in the maximum rotational/carrying speed.

We constructed a straight noncontact carrying road with desktop dimensions to transport a substrate composed of polysilicon wafers having dimensions of 150(W) × 150(L) × 0.3(t). The carrying speed increased with decreased clearance.

ACKNOWLEDGEMENTS

This study was supported by a 2005 Industrial Technology Research Grant Program from Japan's New Energy and Industrial Technology Development Organization (NEDO).

REFERENCES

1. Jin, J., Jeon, J. and Higuchi, T., "Direct Electrostatic Levitation and Propulsion of Silicon Wafer," IEEE IAS 31st Annual Meeting, 1996.

2. Hu, J., Nakamura, K. and Ueha, S., "An Analysis of a Noncontact Ultrasonic Motor with an Ultrasonically Levitated Rotor," Ultrasonics, Vol. 35, pp. 459–467, 1997.

3. Hu, J., Yamazaki, T., Nakamura, K. and Ueha, S., "Analysis of an Ultrasonic Motor Driving Fluid Directly," Japanese Journal of Applied Physics, Vol. 34, pp. 2702–2706, 1995.

4. Taguchi, M., Koike, Y., Nakamura, K. and Ueha, S., "Simplification of a Non-contact High Speed Ultrasonic Motor with a Levitated Rotor," Technical Report of the IEICE, US99-11, pp. 21–26, 1999.

5. Hashimoto, Y., Koike, Y. and Ueha, S., "Acoustic Levitation of Planae Objects Using a Longitudinal Vibration Mode," Journal of the Acoustical Society of Japan (E), Vol. 16, No. 3, pp. 189–192, 1995.